Two-point correlation function for the triangular Ising antiferromagnet

David H. Wojtas and R. P. Millane*
Computational Imaging Group, Department of Electrical and Computer Engineering, University of Canterbury, Private Bag 4800, Christchurch, New Zealand

(Received 6 May 2008; published 15 April 2009; publisher error corrected 5 June 2009)

A number of aspects of the two-point correlation behavior of the nearest-neighbor, triangular Ising antiferromagnet are studied using a combination of numerical evaluation of exact expressions and Monte Carlo simulation. Existing asymptotic results for on-axis correlations at finite temperatures are evaluated and shown to be of limited accuracy. The sublattice structure of the off-axis correlation function is clarified, and rotational invariance is studied as a function of temperature. Separations and temperatures for which the correlation function is significant are identified, and a simple functional expression is developed that allows accurate calculation of the correlation function in this region.

DOI: 10.1103/PhysRevE.79.041123 PACS number(s): 05.50.+q, 75.10.Hk

I. INTRODUCTION

The classical triangular Ising antiferromagnet (TIA) is of considerable interest as it is an archetypical geometrically frustrated system. Geometric frustration results from the inability of a system to satisfy all bonds due to the topology of the underlying lattice. Such systems have a highly degenerate ground state, exhibiting residual ground state entropy. Geometric frustration is increasingly being recognized as an important organizing principle in systems from a diverse range of areas, including coding theory, spin glasses, superconducting networks, quantum dynamics, protein folding, and neural computation [1–6]. The correlation behavior of the TIA provides a basic description of its cooperative properties, and an accurate description of the correlation function is useful in some applications. Despite considerable study, however, a number of aspects of the correlation function of the TIA, including convenient and accurate computation, are poorly understood. In this paper we address a number of these aspects of the correlation function for the TIA.

The TIA partition function was first evaluated by including diagonal interactions in the transfer matrix diagonalization method of Onsager [7–11]. A simpler alternative to Onsager's algebraic method of solution is the combinatorial method formulated by Kasteleyn [12]. This approach utilizes a number of topological theorems to reduce the calculation to a problem of counting dimer coverings, the combinatorics of which can be described by a mathematical object known as a Pfaffian. Stephenson implemented this method to evaluate the TIA partition function, reproducing earlier results as well as obtaining different insights into the system [13].

Another advantage of the Pfaffian approach is that it admits a straightforward calculation of correlation functions. Montroll, Potts, and Ward showed that for on-axis separations the two-point correlation function of the square lattice Ising model reduces to a Toeplitz determinant [14]. Stephenson later performed an analogous calculation for the TIA, from which he developed an approximate expression for the correlation function at zero temperature [13]. The results can also be obtained using spinor algebra, although the analysis is in general more complicated [7]. Utilizing the theory of Toeplitz determinants developed by Wu [15], Stephenson also obtained asymptotic information on the on-axis correlation function for finite temperatures [16].

Adapting the Pfaffian technique to the calculation of off-axis correlations has proven to be a nontrivial task, as foreseen by Montroll *et al.* [14]. Even so, asymptotic information has been obtained for the square Ising model [17]. Alternative approaches to calculating correlations have been developed for the square Ising model, most utilizing connections between statistical physics and quantum field theory [18–20]. However, little progress has been made in adapting these methods to the triangular lattice.

Although, as outlined above, much is known about the correlation behavior of the TIA, there are some significant gaps. For on-axis pairs of sites and at zero temperature, the elements of the Toeplitz determinant are easily evaluated and accurate approximations to the determinant have been developed [13]. For nonzero temperatures, the elements of the determinant are not easily evaluated, and although asymptotic expansions have been developed, their precision has not been investigated. At zero temperature the on-axis correlation function can be partitioned into three sublattices with smoothly varying dependence on separation in each. To leading order, the correlation functions on two of the sublattices become degenerate. For nonzero temperature, the leading order degenerate behavior is evident only for sufficiently small temperatures. The higher order nondegenerate behavior, although certainly present, has not been shown to follow from the asymptotic expansions. For pairs of sites not on a lattice axis, much less is known rigorously. Results for the triangular solid-on-solid (SOS) model [21] and structure factor calculations [22] indicate that the correlation function is rotationally invariant to leading order and for sufficiently small temperatures. (This is in contrast to, for example, the brick lattice for which the correlations are anisotropic [23].) These results only address the leading order degenerate sublattice case, however. There are no results for the off-axis correlation function at higher order that are necessary to accurately describe correlation coefficients for small separations. Furthermore, there are no results for off-axis correlations at higher temperatures.

*rick.millane@canterbury.ac.nz

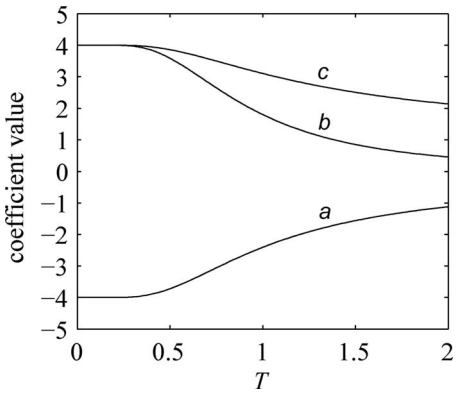

FIG. 1. Coefficients a, b, and c vs temperature.

In this paper we address some of the shortcomings in current knowledge of the correlation function for the TIA. This is achieved through a combination of known exact results for the on-axis case at $T=0$, numerical integration of known analytic expressions at finite temperature, and through Monte Carlo simulation for off-axis separations. We evaluate the precision of existing approximations for the on-axis case at zero and finite temperatures. The off-axis case is examined in some detail. It is noted that the sublattice description that has been employed to partition the correlation function at leading order is not suitable for a higher order description of the correlation function. Rotational invariance is studied and evaluated as a function of temperature. The region of separation-temperature space in which correlations are significant is identified. Finally, expressions are developed that allow accurate calculation of correlation coefficients within this region.

The on-axis correlation function is considered in Sec. II. Exact results are reviewed and the precision of existing approximations is evaluated. The off-axis correlation function is studied in Sec. III, and the sublattice structure and rotational invariance are examined in detail. In Sec. IV the region of separation-temperature space where the correlation function has significant value is determined and a simple expression for the correlation function is developed. Concluding remarks are made in Sec. V.

II. ON-AXIS CORRELATION FUNCTION

The isotropic TIA with nearest-neighbor interactions is defined by the Hamiltonian

$$H = -J\sum_{k}\sum_{l}\left(s_{kl}s_{k+1,l} + s_{kl}s_{k,l+1} + s_{kl}s_{k+1,l+1}\right), \tag{1}$$

where $s_{kl}=\pm 1$ are the Ising spins, (k,l) indexes the sites on the triangular lattice, and $J<0$ is the antiferromagnetic bond strength between nearest neighbor spins. The TIA has a critical point at $T=0$ where it is fully frustrated. We use a rescaled temperature parameter $\tilde{T}=k_BT/|J|$ and, for brevity, we rewrite $\tilde{T}$ as T.

By applying the Pfaffian technique of Montroll *et al.* [14], Stephenson [13] showed that for on-axis separations the TIA two-point correlation function is given by the Toeplitz determinant

$$\rho_{k0} \equiv \langle s_{00}s_{k0}\rangle = \begin{vmatrix} a_0 & a_1 & a_2 & \cdots & a_{k-1} \\ a_{-1} & a_0 & a_1 & \cdots & a_{k-2} \\ a_{-2} & a_{-1} & a_0 & \cdots & a_{k-3} \\ \vdots & \vdots & \vdots & \cdots & \vdots \\ a_{1-k} & a_{2-k} & a_{3-k} & \cdots & a_0 \end{vmatrix}, \tag{2}$$

where $\langle\cdot\rangle$ is the ensemble average over all configurations. The elements a_n are given by [13]

$$a_n = \frac{1}{2\pi}\int_{-\pi}^{\pi} e^{-in\omega}\left(\frac{a-be^{i\omega}+ce^{-i\omega}}{a-be^{-i\omega}+ce^{i\omega}}\right)^{1/2} d\omega, \tag{3}$$

where, for the isotropic lattice,

$$a = 2\nu(1+\nu^2), \quad b = \nu^2(1-\nu)^2, \quad c = (1-\nu)^2, \tag{4}$$

with $\nu=\tanh K$ and $K=-1/T$.

A. Ground state

At zero temperature, the integrand of Eq. (3) simplifies, allowing the integral to be performed, giving [13]

$$a_n = \begin{cases} -1/3, & n=0 \\ 0, & n=3r \\ \sqrt{3}/(\pi n), & n=3r-1 \\ -\sqrt{3}/(\pi n), & n=3r-2, \end{cases} \tag{5}$$

where $r=1,2,\ldots$. Exact correlation values can then be calculated by substituting Eq. (5) into Eq. (2) and evaluating the determinant.

An interesting result of the above calculation is that any given lattice site is negatively correlated to its first and second nearest neighbors and positively correlated to its third nearest neighbor. This pattern then repeats along the axis such that every third spin is positively correlated with the origin spin. By numerical fitting of exact correlation values calculated from Eq. (2), Stephenson [13] obtained the asymptotic approximations

$$\rho_{k0} \simeq \begin{cases} \epsilon_0 k^{-1/2} + \epsilon_2 k^{-5/2} + \ldots, & k=0,3,6\ldots \\ (-\epsilon_0/2)k^{-1/2} + \epsilon_1 k^{-3/2} + \ldots, & k=1,4,7\ldots \\ (-\epsilon_0/2)k^{-1/2} - \epsilon_1 k^{-3/2} + \ldots, & k=2,5,8\ldots, \end{cases} \tag{6}$$

where $\epsilon_0=0.632\,226(2)$, $\epsilon_1=0.32(2)$, and $\epsilon_2=-0.187(5)$. The form of Eq. (6) indicates that the on-axis sites can be partitioned into three sublattices, each of three times the lattice spacing, with the correlations in each sublattice being described by the three expressions in Eq. (6). The sublattice that contains the origin has positive correlations and the other two have negative correlations. For large k, all correlations decay as $k^{-1/2}$ and the two sets of negative correlations have the same form. To leading order then, all on-axis correlations can be expressed as

$$\rho_{k0} \simeq \epsilon_0 k^{-1/2} \cos\left(\frac{2\pi k}{3}\right), \tag{7}$$

where the cosine takes the value +1 or −1/2 depending on whether the sublattice to which k belongs contains the origin or does not, respectively. Hence, to leading order, the two sublattices that do not contain the origin become degenerate and the correlation coefficient falls into one of two classes. For small k the higher order terms are significant, however.

B. Finite temperature

At finite temperature, Eq. (3) is not solvable except in a few limiting cases where it may be reduced to a form in terms of elliptic integrals [24]. Using asymptotic properties of the Toeplitz determinant [15], Stephenson [16] obtained an asymptotic expansion in k for the correlation function ρ_{k0} at finite temperature. The first two terms of this expansion are

$$\begin{aligned}\rho_{k0} \sim & \left(\frac{\pi}{2}\sin\theta\right)^{-1/2} \nu^k k^{-1/2} \left\{ \cos\left(k\theta + \frac{\theta}{2} - \frac{\pi}{4} - \phi\right) \right. \\ & - (4k)^{-1} \left[\frac{3}{2} + (2\sin\theta)^{-1} \cos\left(k\theta + \frac{3\theta}{2} + \frac{\pi}{4} - \phi\right) \right. \\ & + \nu^2 (1-\nu^2)^{-1} \cos\left(k\theta + \frac{\theta}{2} - \frac{\pi}{4} - \phi\right) \\ & \left. \left. + \nu^2 \rho^2 \cos\left(k\theta + \frac{5\theta}{2} - \frac{\pi}{4} - 3\phi\right) \right] \right\}, \end{aligned} \tag{8}$$

where $\theta = \cos^{-1}[(1+\exp 4K)/2]$, $\rho = (1 - 2\nu^2 \cos 2\theta + \nu^4)^{-1/4}$, and $\phi = \arg(1 - \nu^2 \cos 2\theta + i\nu^2 \sin 2\theta)/2$. The calculation utilizes the similarity between a Toeplitz determinant and the Wiener-Hopf sum equation which only holds when k (and hence the size of the Toeplitz determinant) is large, and when $T \gg 0$. By the use of Szego's theorem, the asymptotic behavior of the Toeplitz determinant as $k \to \infty$ can be inferred. Equation (8) is therefore expected to break down for small k, and also for $T \to 0$.

It is useful to examine the behavior of Eq. (8) for $T \to 0$. With $T=0$, $\nu=-1$, $\theta=\pi/3$, $\rho=3^{-1/4}$, and $\phi=-\pi/12$. Substitution into Eq. (8) shows that the term of order $k^{-3/2}$ diverges as a result of the factor $(1-\nu^2)^{-1}$. The first term remains finite however, and to leading order Eq. (8) reduces to

$$\begin{aligned}\rho_{k0} &\sim (2\pi^{-1/2} 3^{-1/4}) k^{-1/2} \cos\left(\frac{2\pi k}{3}\right) \\ &\sim (0.8753) k^{-1/2} \cos\left(\frac{2\pi k}{3}\right). \end{aligned} \tag{9}$$

Comparison with Eq. (7) shows the same functional form but a discrepancy between the prefactors of 0.8753 vs $\epsilon_0 = 0.632\,226$.

C. Numerical integration

The on-axis correlation coefficients for $T > 0$ were calculated by writing Eq. (3) in the real form

$$a_n = \frac{1}{\pi} \int_0^\pi \frac{\cos(n\omega)(a - b\cos\omega - c\cos\omega) + \sin(n\omega)(-b\sin\omega + c\sin\omega)}{[a^2 + b^2 + c^2 - 2a(b+c)\cos\omega + 2bc\cos(2\omega)]^{1/2}} d\omega, \tag{10}$$

integrating it numerically and evaluating the determinant. Numerical integration was performed using an adaptive Gauss-Lobatto quadrature algorithm described in Ref. [25], using an error tolerance of 1×10^{-6}. Calculations were repeated using various tolerance values and the results showed that the above value is sufficient. We note that for $n=1$, Eq. (10) can be evaluated in terms of complete elliptic integrals [24], although the resulting expression is not convenient for numerical evaluation.

D. Approximations

Before results from numerical integration are presented, we discuss the qualitative information available from the variation of the coefficients a, b, and c of Eq. (4) with T, which is shown in Fig. 1. Inspection of the figure shows that for T less than about 0.3 there is little variation in their values. This suggests that there will be little variation in the correlation function in the interval $0 \leqslant T \lesssim 0.3$. As $T \to \infty$, $\nu \to 0$, so that $a \to 0$, $b \to 0$, and $c \to 1$. Substituting into Eq. (3) shows that $a_n \to 0$ and from Eq. (2) $\rho_{k0} \to 0$, i.e., the system is completely disordered, as expected.

The correlation function at $T=0$ was calculated on the interval $1 \leqslant k \leqslant 20$ using Eqs. (2) and (5) and is shown by the filled circles in Fig. 2. We refer to these values as "exact." The positive and negative correlations as described above are evident. Close inspection of the figure shows that for small k, the negative correlations fall on two smooth curves as described above, but the difference between the two curves is small for $k \gtrsim 10$. The approximation Eq. (7) was calculated and is shown as the crosses in Fig. 2. The maximum absolute error of the approximation is 0.03 and the maximum relative error 0.15. Both errors decrease with increasing k. The approximation Eq. (9) was also calculated and was found to be less accurate than Eq. (7). The prefactor 0.8753 derived for finite temperatures is therefore inappropriate for the ground state. Including the second order terms in Eq. (6) gives a better approximation with a maximum error of about 0.01. The correlation function was also calculated using numerical integration of Eq. (10) and the results agree with the exact

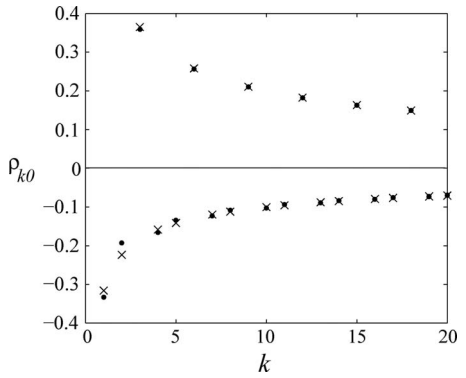

FIG. 2. On-axis correlation function at $T=0$ calculated using Eq. (2) and Eq. (5) (•), and using the approximation Eq. (7) (×).

values with an error of less than 3×10^{-5}. This indicates that the adaptive quadrature method is suitable for calculating accurate correlation functions for $T>0$ where the a_n cannot be determined analytically. Since high precision values of ρ_{k0} may be useful for other studies, the values of ρ_{k0} calculated by numerical integration are listed Table I. We note in passing that the correlation coefficients presented in Table II of Ref. [13] are in error, although the estimate of ϵ_0 is correct.

For finite temperature, the correlation function was calculated using Eq. (2) and numerical integration of Eq. (10). Given the precision of the numerical integration, these results are treated as exact. Results are shown by the filled

TABLE I. Values of ρ_{k0} for $T=0$, 0.5, 1.0, and ρ_{kk} for $T=0$.

k	$\rho_{k0}(T)$[a] $T=0$	$T=0.5$	$T=1.0$	$\rho_{kk}(T)$[b] $T=0$
0	1	1	1	1
1	−0.33333	−0.33243	−0.31038	0.487
2	−0.19285	−0.18652	−0.10865	0.344
3	0.35852	0.34387	0.19067	0.282
4	−0.16561	−0.15734	−0.08130	0.241
5	−0.13362	−0.12079	−0.03266	0.219
6	0.25682	0.22977	0.06288	0.199
7	−0.12320	−0.10900	−0.02898	0.184
8	−0.10801	−0.09003	−0.01100	0.173
9	0.21026	0.17335	0.02308	0.163
10	−0.10225	−0.08333	−0.01125	0.154
11	−0.09302	−0.07094	−0.00388	0.147
12	0.18227	0.13749	0.00888	0.140
13	−0.08925	−0.06656	−0.00454	0.135
14	−0.08290	−0.05756	−0.00139	0.131
15	0.16311	0.11205	0.00351	
16	−0.08020	−0.05449	−0.00188	
17	−0.07549	−0.04756	−0.00050	
18	0.14893	0.09288	0.00141	
19	−0.07344	−0.04532	−0.00079	
20	−0.06977	−0.03978	−0.00018	

[a]The precision of ρ_{k0} is 3×10^{-5}.
[b]The precision of ρ_{kk} is 5×10^{-3}.

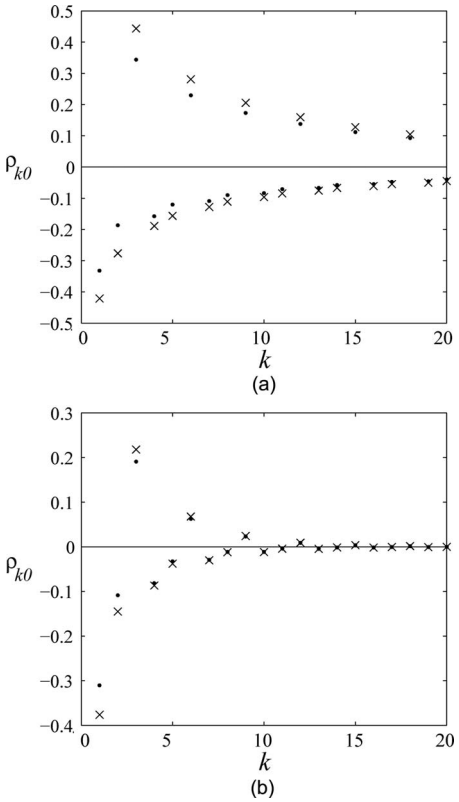

FIG. 3. On-axis correlation function calculated exactly by numerical integration (•) and from the first term of Eq. (8) (×) for (a) $T=0.5$ and (b) $T=1.0$.

circles in Fig. 3 for $T=0.5$ and $T=1.0$. The negative correlations fall on two smooth curves here also. The correlation coefficient falls off more rapidly with k for increasing T as expected. The short-range correlations are shown vs temperature in Fig. 4. They are seen to be approximately constant for $T\leqslant0.3$ as anticipated above. The correlations were also calculated using the first term of the asymptotic expansion Eq. (8) and are shown by the crosses in Fig. 3. The maximum absolute error is 0.11 and the maximum relative error 0.48 for $T=0.5$, and are larger for smaller temperatures, as expected. Note, however, particularly for $T=1.0$, that the approximate expression also describes two smooth curves for the negative correlations, in distinction to the leading order

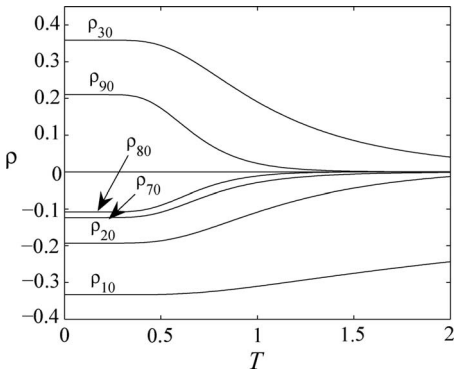

FIG. 4. Low-order on-axis correlation coefficients vs temperature.

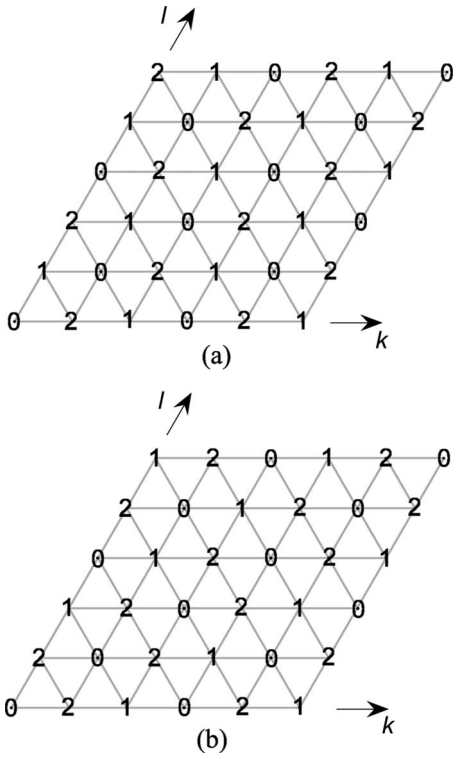

FIG. 5. The sublattice partitioning implied by (a) Eq. (7) and (b) Eq. (6). The origin is at lower left vertex.

Eq. (7) for $T=0$. Including the second term, of order $\mathcal{O}(k^{-3/2})$, in Eq. (8) gives a less accurate approximation, particularly for small T, as anticipated above. Equation (8) is therefore unsuitable for high precision calculation of the correlation function. The values of ρ_{k0} calculated by numerical integration for $T=0.5$ and 1.0 are listed in Table I.

III. OFF-AXIS CORRELATION FUNCTION

The correlation coefficient for two sites, not necessarily lying on a lattice axis, is denoted by $\rho_{kl}=\langle s_{00}s_{kl}\rangle$. Little is known rigorously concerning the coefficients ρ_{kl}. An important question is the extent to which ρ_{kl} is rotationally invariant, i.e., depends only on the distance,

$$r_{kl}=(k^2+l^2+kl)^{1/2}, \tag{11}$$

between the sites (0,0) and (k,l). Some information on the nature of ρ_{kl} has been obtained by Nienhuis *et al.* [21] who mapped the TIA with a staggered field onto a period-6 spin wave operator of the triangular solid-on-solid model. Their work indicates that at $T=0$, and for $r_{kl}\gg 1$, ρ_{kl} is expected to follow Eq. (7) with the separation k replaced by r_{kl} and the cosine term replaced by a weight factor equal to +1 when (k,l) belongs to a sublattice of the form $(3m+n,n)$, for all integers m and n, and $-1/2$ otherwise. This behavior can be described by partitioning the triangular lattice into three sublattices, labeled 0, 1, and 2, as shown in Fig. 5(a), fixing the origin on sublattice 0, and partitioning the correlation function ρ_{kl} into two sets, one for which the site (k,l) is on sublattice 0, and the other for which it is on sublattice 1 or 2.

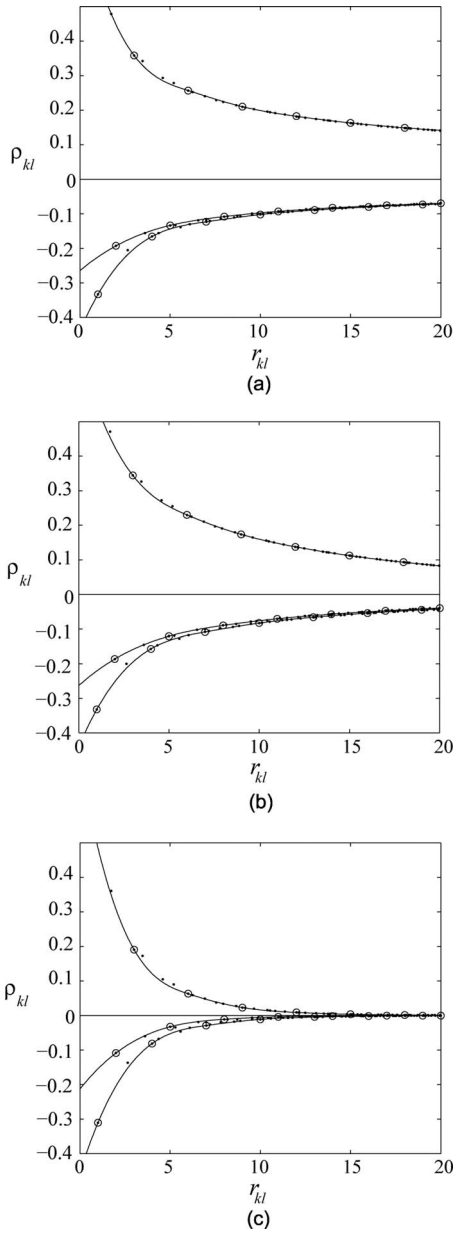

FIG. 6. On-axis correlation coefficients ⊙ with spline interpolation (-), and off-axis correlation coefficients calculated by MC simulation, (•), for (a) $T=0$, (b) $T=0.5$, and (c) $T=1.0$. The three curves are for the three sublattices.

The sublattices 0, 1, and 2 can be indexed by the sites $(3m+n,n)$, $(3m-1+n,n)$, and $(3m+1+n,n)$, respectively, for all integers m and n. Since the form of the off-axis correlation function as described above is identical on sublattices 1 and 2, we say that it is degenerate with respect to these two sublattices. Monte Carlo calculations of structure factors support this contention for sufficiently small temperatures [22]. The off-axis correlation function for larger temperatures has not been studied.

The results described above address only the leading order behavior of the off-axis correlation function. In this section we study the structure of the off-axis correlations using high precision Monte Carlo calculations, and the degree to which they are rotationally invariant.

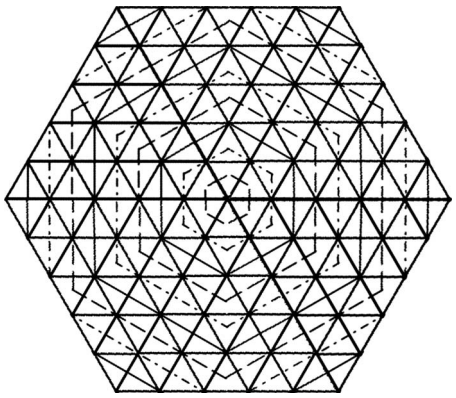

FIG. 7. A representation of the sublattice structure of the TIA corresponding to Fig. 5(b) that describes the correlations of the TIA. The full-line hexagons pass through the sites of sublattice 0, and the dash-dot hexagon through the sites of sublattice 1, and the dashed line hexagon through the sites of sublattice 2.

A. Monte Carlo simulation

Since analytical results are not available for calculating the off-axis correlation coefficients for the TIA, they were calculated using Monte Carlo (MC) simulation. Since MC simulation near the ground state and for frustrated systems can be difficult, our methods are briefly outlined here. MC simulation was performed using an algorithm developed specifically for the TIA model [26,27]. It employs the Kandel–Ben-Av–Domany (KBD) framework for zero-temperature MC simulation of fully frustrated Ising models [28]. This framework is very efficient at low temperatures where the Metropolis algorithm [29] suffers from critical slowing, and where the Swendsen-Wang algorithm [30] becomes trivial by freezing the entire lattice into a single cluster. The algorithm is outlined briefly here and the reader is referred to Ref. [27] for more details. The KBD cluster algorithm combines elements of the Metropolis and Swendsen-Wang algorithms. First, the lattice is partitioned into two sets of triangular plaquettes, one of which is chosen at random for each Monte Carlo step. Bonds between spins are then labeled as "frozen" or "deleted" depending on the orientation of spins in the plaquette and strict criteria to satisfy the condition of detailed balance. A frozen bond is added to a cluster of connected bonds, and a deleted bond is not. If all three bonds in a plaquette are unsatisfied, all three bonds are deleted. If two bonds are satisfied, then all three bonds are deleted with probability $p=\exp(4K)$. If this does not occur, then one of the two satisfied bonds is chosen with probability $p=1/2$ and then frozen with probability $p=1-\exp(4K)$, while the other two bonds are deleted. Clusters of connected frozen bonds are then flipped in a Swendsen-Wang manner, bringing about large steps in configuration space. A Metropolis sweep is then performed to ensure that the simulation is ergodic.

The TIA was simulated on an $L\times L$ lattice on a rhombic domain with toroidal boundary conditions. We used L as a multiple of 6 to avoid dislocations in sublattice configurations across the boundaries, and generally $L=300$. Thermalization times used were generally 1×10^5 sweeps. Decorrelation times τ were calculated and correlation values calculated by sampling every τ sweeps and averaging over 2×10^4 samples. Standard deviations of correlation coefficients calculated from the MC simulations were typically about 5×10^{-4}. Comparison of on-axis correlation coefficients with those calculated by numerical integration gave a maximum absolute difference of 3×10^{-3}.

TABLE II. Pairs (k,l) and (k',l') that lie on the same sublattice and such that $r_{kl}=r_{k'l'}$, used to study rotational invariance.

Label	Sublattice	r_{kl}^2	(k,l)	(k',l')
A	0	147	(11,2)	(7,7)
B	2	169	(13,0)	(8,7)
C	2	217	(13,3)	(9,8)
D	0	273	(16,1)	(11,8)
E	1	301	(15,4)	(11,9)
F	0	399	(17,5)	(13,10)
G	1	403	(19,2)	(14,9)
H	0	441	(21,0)	(15,9)

B. Rotational invariance

The degree to which ρ_{kl} is rotationally invariant is of fundamental interest, and is also of interest because it would simplify the description of the correlation function. Note first that the correlation function must satisfy the symmetry relationships

$$\rho_{kl}=\rho_{lk}=\rho_{-l,k}=\rho_{l,-k}=\rho_{-k,-l}. \tag{12}$$

It is therefore sufficient to study ρ_{kl} in the sector $S=\{(k,l):k\geqslant 0,0\leqslant l\leqslant k\}$, as all other values can be generated from these using Eq. (12).

Rotational invariance is first assessed by interpolating (using cubic splines with "not-a-knot" end conditions) the on-axis correlation coefficients as a function of r_{kl} within each of the three sublattice groups described in Sec. II, and comparing the off-axis correlations calculated by MC simulation with the interpolated values at the same value of r_{kl}. The results are shown for three temperatures in Fig. 6 and the off-axis values are seen to fit well to the interpolated values. This indicates that the on- and off-axis correlations can probably be quite accurately described by three functions of the distance r_{kl} between sites. This is addressed further in Sec. IV. Inspection of Fig. 6 shows that the off-axis correlations fall onto the three curves defined by the on-axis correlations. Inspection of the indices (k,l) corresponding to points on the three curves shows that they correspond to the three sublattices described above, but only within the sector S. Note that now, because the functional form of the correlation is different on sublattices 1 and 2, the off-axis correlations are not degenerate with respect to these two sublattices. Therefore to describe the correlation function outside the sector S, the symmetry relationships Eq. (12) must be applied to the partitioning in S, which gives the full partitioning shown in Fig. 5(b). This partitioning describes the correlations relative to an origin on sublattice 0. Note the difference between Figs. 5(a) and 5(b). Although the partitions 1 and 2 in Fig. 5(b) do

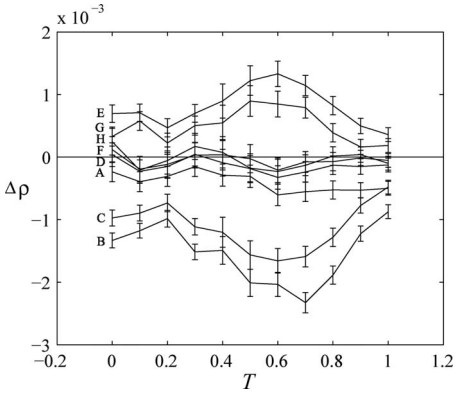

FIG. 8. Differences in correlation coefficients for different lattice separations with the same radial distance as described in the text. Vertical bars show ±1 standard deviation. The different curves are defined in Table II.

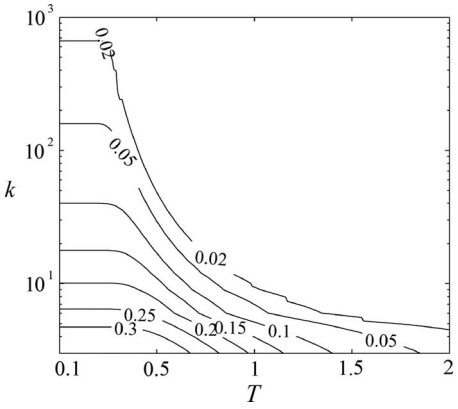

FIG. 9. Contour plot of $\rho_{3k,0}$ vs k (on a log scale) and T.

not have translational symmetry, we refer to them, for convenience, as sublattices. The correlations are therefore determined not by being "on" or "off" a sublattice, but by their membership of sublattice 0, 1, or 2, relative to an origin on sublattice 0. The sublattices can be described in terms of sets of hexagons as shown in Fig. 7. The values of ρ_{kk} for $T=0$ and out to $r_{kk}=20$ are listed in Table I.

Since ρ_{kl} is a function of the discrete variables k and l, strict rotational invariance would imply that for a particular T, $\rho_{kl}=\rho_{k'l'}$ for all (k,l) and (k',l') belonging to the same sublattice and for which $r_{kl}=r_{k'l'}$. The degree to which the correlations are rotationally invariant was therefore further studied by calculating and comparing correlation coefficients for pairs of sites (k,l) and (k',l') with the same radius and on the same sublattice. Eight such pairs listed in Table II were tested and the difference $\Delta\rho=\rho_{kl}-\rho_{k'l'}$ between the correlation coefficients in each pair are plotted vs temperature in Fig. 8. Increasing the lattice size beyond $L=300$ made no significant difference to the values of $\Delta\rho$. The results show that although rotational invariance is not satisfied exactly, deviations from rotational invariance are less than 2×10^{-3}. The results in Fig. 8 are suggestive of the nature of the deviations from rotational invariance but we do not pursue this here.

IV. FUNCTIONAL APPROXIMATION

The results in the previous section indicate that ρ_{kl} can be written approximately in the form

$$\rho_{kl} \simeq \tilde{\rho}(r_{kl},\sigma_{kl}), \tag{13}$$

where σ_{kl} depends *only* on the sublattice to which (k,l) belongs. They also indicate that the off-axis correlation coefficients can be obtained by interpolation from the on-axis coefficients. The latter can be obtained by evaluating Eqs. (2) and (10), although this is not particularly convenient. Here we develop simple expressions that can be used to calculate the correlation function over a range of values of k and T. Since the correlation function is largest on the 0 sublattice, the range of values of k and T for which the correlation has significant value is determined by calculating $\rho_{3k,0}$ vs k and T. The results are shown as a contour plot in Fig. 9. We chose (arbitrarily) to describe $\rho_{kl}(T)$ in the region for which $\rho_{kl}(T)<0.02$. This is done by developing suitable functions $\rho(r_{kl},T)$ and fitting them to the on-axis values obtained from Eqs. (2), (5), and (10), for each sublattice. Off-axis correlations are then obtained by evaluating these expressions for the appropriate value of r_{kl}. A suitable expression was developed as follows.

We know that for $T=0$ the on-axis correlation function behaves approximately as $k^{-1/2}$. Although the leading order behavior is not particularly accurate for small k, this can potentially be improved by allowing the prefactor ϵ_0 in Eq. (7) to vary between the sublattices. For finite temperature, to leading order [Eq. (8)], in addition to the $k^{-1/2}$ dependence, there is an exponential decay through the factor ν^k. The temperature dependence is primarily through the temperature dependence of ν, but there is also an effect on the prefactor

TABLE III. Values of the coefficients $\alpha_i(T)$ and $\beta(T)$ to an accuracy of 10^{-3}, and the correlation length.

	$\alpha_i(T)$				
T	$i=0$	$i=1$	$i=2$	$\beta(T)$	$\xi(T)$
0	0.623	−0.298	−0.326	1.000	∞
0.1	0.623	−0.298	−0.326	1.000	$>10^3$
0.2	0.623	−0.298	−0.326	1.000	$>10^3$
0.3	0.642	−0.295	−0.336	0.998	499.5
0.4	0.655	−0.292	−0.339	0.989	90.4
0.5	0.667	−0.289	−0.345	0.969	31.8
0.6	0.678	−0.284	−0.353	0.939	15.9
0.7	0.690	−0.279	−0.362	0.902	9.7
0.8	0.700	−0.272	−0.371	0.860	6.6
0.9	0.709	−0.265	−0.380	0.816	4.9
1.0	0.716	−0.258	−0.389	0.773	3.9
1.1	0.722	−0.251	−0.399	0.731	3.2
1.2	0.728	−0.244	−0.408	0.691	2.7
1.3	0.733	−0.240	−0.417	0.653	2.3
1.4	0.738	−0.240	−0.426	0.617	2.0
1.5	0.742	−0.240	−0.434	0.584	1.8

through the cosine term in Eq. (8). It was found that the form ν^k was insufficient to accurately describe the temperature dependence, so ν was replaced by a general function of T. In summary then, an expression of the form

$$\rho(r,T) = \alpha_i(T) r^{-1/2} [\beta(T)]^r \tag{14}$$

is used as a tentative description of the correlation function, where for convenience we have replaced r_{kl} by r, the coefficients α_i and β depend on temperature, and α_i depends on the sublattice i. As $T \to 0$ we expect $\beta \to 1$ and α_0 to approach ϵ_0. Note that the cosine factor in Eqs. (7) and (8) has been absorbed into α_i. Note also that writing Eq. (14) in the form $\rho(r,T) = \alpha_i(T) r^{-1/2} e^{-r/\xi(T)}$ shows that $\xi(T) = -1/\ln[\beta(T)]$ is a correlation length, and that $\xi(T) \to \infty$ as $T \to 0$. The coefficients $\alpha_i(T)$ and $\beta(T)$ were determined by making a least-squares fit of Eq. (14) to the on-axis correlation function over $0 \leqslant r \leqslant 700$ (for which the correlation function is less than 0.02) for $0 \leqslant T \leqslant 1.5$ with an interval of 0.1.

The resulting coefficients are listed in Table III. The mean and maximum absolute errors in the fit for all the correlations (on-axis and off-axis) are 5×10^{-3} and 0.017, respectively. The maximum relative error in the fit is 0.11. For intermediate temperatures, linear interpolation of the coefficients in Table III gives equivalent precision. For interest, the correlation length $\xi(T)$ is also listed in Table III. Because of the precision with which β can be estimated, only a lower bound can be obtained for ξ for $T \leqslant 0.2$. Of course the correlation length continues to grow throughout this temperature range. In summary, Eq. (14), together with the coefficients listed in Table III, allows convenient and accurate calculation of the on- and off-axis correlation function in the region specified above.

V. CONCLUSIONS

The correlation behavior of the triangular Ising antiferromagnet has been studied in detail through numerical evaluation of exact analytical results and Monte Carlo simulation. The precision of existing approximations for on-axis correlations for finite temperatures, are found to be unsuitable for high precision calculations. A lattice partitioning is defined that describes the symmetry of high precision off-axis correlations. The correlation function is shown to be not exactly rotationally invariant at all temperatures, but to be approximately rotationally invariant within a given small error. This allows an accurate description of the correlation function in terms of only radial separation and the sublattice. The region of separation-temperature space where correlations are significant is identified, and simple approximations are derived that accurately describe the correlation function in this region. These latter expressions will be useful to those using the TIA to quantitatively model various systems.

[1] G. Aeppli and P. Chandra, Science **275**, 177 (1997).
[2] D. Davidovic, S. Kumar, D. H. Reich, J. Siegel, S. B. Field, R. C. Tiberio, R. Hey, and K. Ploog, Phys. Rev. B **55**, 6518 (1997).
[3] R. Moessner and S. L. Sondhi, Phys. Rev. B **63**, 224401 (2001).
[4] A. P. Ramirez, Nature (London) **421**, 483 (2003).
[5] M. Mezard, Science **301**, 1685 (2003).
[6] R. F. Wang, C. Nisoli, R. S. Freitas, J. Li, W. McConville, B. J. Cooley, M. S. Lund, N. Samarth, C. Leighton, V. H. Crespi, and P. Schiffer, Nature (London) **439**, 303 (2006).
[7] L. Onsager, Phys. Rev. **65**, 117 (1944).
[8] L. Wannier, Phys. Rev. **79**, 357 (1950).
[9] R. M. F. Houtappel, Physica (Amsterdam) **16**, 425 (1950).
[10] K. Husimi and I. Syôzi, Prog. Theor. Phys. **5**, 177 (1950).
[11] G. F. Newell, Phys. Rev. **79**, 876 (1950).
[12] P. W. Kasteleyn, J. Math. Phys. **4**, 287 (1963).
[13] J. Stephenson, J. Math. Phys. **5**, 1009 (1964).
[14] E. W. Montroll, R. B. Potts, and J. C. Ward, J. Math. Phys. **4**, 308 (1963).
[15] T. T. Wu, Phys. Rev. **149**, 380 (1966).
[16] J. Stephenson, J. Math. Phys. **11**, 413 (1970).
[17] H. Cheng and T. T. Wu, Phys. Rev. **164**, 719 (1967).
[18] T. T. Wu, B. M. McCoy, C. A. Tracy, and E. Barouch, Phys. Rev. B **13**, 316 (1976).
[19] V. S. Dotsenko and V. S. Dotsenko, Adv. Phys. **32**, 129 (1983).
[20] V. N. Plechko, Physica A **152**, 51 (1988).
[21] B. Nienhuis, H. J. Hilhorst, and H. W. J. Blote, J. Phys. A **17**, 3559 (1984).
[22] J. L. Jacobsen and H. C. Fogedby, Physica A **246**, 563 (1997).
[23] C. S. O. Yokoi, J. F. Nagle, and S. R. Salinas, J. Stat. Phys. **44**, 729 (1986).
[24] T. C. Choy, J. Math. Phys. **25**, 3558 (1984).
[25] W. Gander and W. Gautschi, BIT **40**, 84 (2000).
[26] P. D. Coddington and L. Han, Phys. Rev. B **50**, 3058 (1994).
[27] G. M. Zhang and C. Z. Yang, Phys. Rev. B **50**, 12546 (1994).
[28] D. Kandel, R. Ben-Av, and E. Domany, Phys. Rev. Lett. **65**, 941 (1990).
[29] N. Metropolis, A. W. Rosenbluth, M. N. Rosenbluth, A. H. Teller, and E. Teller, J. Chem. Phys. **21**, 1087 (1953).
[30] R. H. Swendsen and J. S. Wang, Phys. Rev. Lett. **57**, 2607 (1986).